An Experimental and Numerical Study of Splitter-Vane Concept for Turbine Rear Structures

Citation for the original published paper (version of record):
Deshpande, S., Vikhorev, V., Goorden, K. et al (2026). An Experimental and Numerical Study of Splitter-Vane Concept for Turbine Rear Structures. Proceedings of the ASME Turbo Expo

(article starts on next page)

Proceedings of ASME Turbo Expo 2026
Turbomachinery Technical Conference and Exposition
GT2026
June 15-19, 2026, Milan, Italy

GT2026-177665

AN EXPERIMENTAL AND NUMERICAL STUDY OF SPLITTER-VANE CONCEPT FOR TURBINE REAR STRUCTURES

Srikanth Deshpande[1], Valentin Vikhorev[2], Kristie Goorden[1], Mattia Ricchi[1], Jonas Larsson[1], Valery Chernoray[2]
[1]GKN Aerospace Sweden AB, 46181 Trollhättan, Sweden
[2]Chalmers University of Technology, 412 96 Gothenburg, Sweden

ABSTRACT

The purpose of this study is to open a path for an ultra-short engine architecture with reduced weight, a shorter shaft, and better fuel efficiency by delivering a novel splitter-vane based TRS design that achieves the above objectives and could result in reduced SFC. The splitter-vane concept also enables flexible configurations towards implementation of hybrid-electric engines, in which the TRS must accommodate the passage of electrical cables.

The work provides the first validation of numerical tools for a novel aerodynamically aggressive TRS with splitter vanes, thereby reducing design risks by providing good comparison to experimental data. The radical splitter-vane TRS concept has, for the first time, been designed by GKN Aerospace Sweden, while being manufactured, assembled, and tested at TRL4 in the world-unique Chalmers LPT–OGV test rig.

Furthermore, this study presents a direct comparison of the aerodynamic performance of the splitter-vane concept against two engine-realistic state-of-the-art TRS designs: one with radial vanes and one with leaned vanes.

Keywords: Turbine rear structure; splitter vane; turbine rear frame; engine exit structure; turbine exhaust casing; tail bearing housing; turbine rear frame; outlet guide vane; lean vane; low-pressure turbine; ultrashort jet engine; hybrid-electric jet engine

NOMENCLATURE

α, swirl	circumferential flow angle, $\tan^{-1}\left(\frac{v_t}{v_x}\right)$, [deg]
β, yaw	radial flow angle, $\tan^{-1}\left(\frac{v_r}{v_x}\right)$, [deg]
C_{P0}	total pressure coefficient, $\frac{P_T-P_{T,\text{ref}}}{P_{T,\text{ref}}-P_{S,\text{ref}}}$, [-]
C_P	static pressure coefficient, $\frac{P_S-P_{S,\text{ref}}}{P_{T,\text{ref}}-P_{S,\text{ref}}}$, [-]
P_S	static pressure, [Pa]
P_T	total pressure, [Pa]
$P_{T,\text{ref}}$	inlet midspan average total pressure, [Pa]
$P_{S,\text{ref}}$	inlet midspan average static pressure, [Pa]
Re	Reynolds number, UH/ν, [-]
v_x, v_r, v_t	axial, radial and circumferential flow velocity components, [m/s]

ABBREVIATIONS

CFD	Computational Fluid Dynamics
HPT	High-Pressure Turbine
LPT	Low-Pressure Turbine
NGV	Nozzle Guide Vane
OGV	Outlet Guide Vane
RANS	Reynolds Averaged Navier–Stokes
SFC	Specific Fuel Consumption
TRS	Turbine Rear Structure

1. INTRODUCTION

Typically, in a geared turbofan jet engine, the exit flow from low-pressure turbine (LPT) has a high mean swirl and a high gradient from root to tip of the flow path. The Turbine Rear Structure (TRS), located downstream of the Low-Pressure Turbine (LPT), has both the aerodynamic function of de-swirling the flow at TRS exit and the structural functions to support the engine's rear bearing and connecting the engine to the aircraft.

There are continuous efforts by researchers and engineers to reduce Specific Fuel Consumption (SFC) by reducing weight and length and/or by reducing the total pressure losses incurred while de-swirling the flow. The splitter-vane TRS is a configuration that can take advantage of both the above-mentioned strategies. This research group has been looking into design solutions to reduce axial chord while monitoring overall losses in TRS. The splitter-vane design configuration is the most recent design attempt and is the topic of discussion in this paper. Furthermore, the splitter-vane concept enables flexible configurations towards implementation of hybrid-electric engines, in which the TRS must accommodate the passage of thick electrical cables – the concept currently under investigation in a Clean Aviation flagship project SWITCH (Sustainable Water-Injecting Turbofan Comprising Hybrid-Electrics).

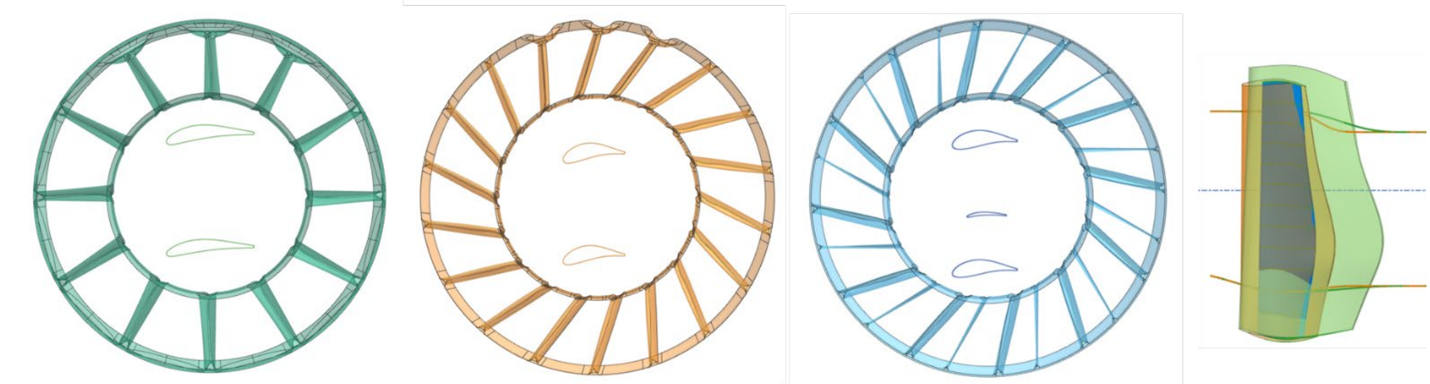

a. Engine Realistic b. Lean vane design c. Splitter vane design

Figure 1 DESIGNS EXPLORED

Early studies on splitter-vane concept on transonic cascades by Youngren et al. [1] were carried out using the numerical tool MISES and experiments. The results from MISES indicated that the circumferential location of the splitter-vane had no effect on loss or turning of flow while the general effect is to reduce the loading on the main blade in the overlapping region. In the context of transonic cascades, the best position for the splitter vane is found to be in a tandem arrangement close to the trailing edge of the main blade resulting in 15% loss reduction.

Another splitter-vane concept was experimentally studied in a low-aspect ratio turbine configuration by Clark et al. [2] and the designs tested were an output from an optimizer-driven process. Three selected splitter-vane designs have been tested, and the measured secondary kinetic energy was reduced by 85% when compared to a reference design with no splitter vanes. Furthermore, the vane row loss was reduced by 6.9% and mixing losses were reduced by 77.4%. The physics that drives the reduction in loss numbers is attributed to reduced secondary mixing losses. The total secondary vorticity is subdivided into smaller vortices resulting in better flow patterns.

A multiple splitter-vane concept in an inter-turbine diffuser connecting a high-pressure turbine (HPT) and a LPT was studied by Yasa et al. [3]. Since the duct consists of low-aspect ratio vanes, secondary losses are dominant. With the objective to reduce such losses, one design configuration with three splitter vanes was tested in a high-speed rotating rig at Von Karman Institute for Fluid Dynamics. To complement the study, numerical simulations are performed on the test object and results are compared with the conclusion that this type of design is reported to lose its performance when the stagnation point moves towards the suction side. At off-design conditions, the performance of splitter-vane concept exhibited some limitation due to incidence issues on the structural vanes.

In the present study, the splitter-vane design concept is explored as a possible solution for a TRS application. The main research objectives for the presented work are:

- Aerodynamic design of a splitter-vane TRS with a shorter axial chord and possibly less weight.
- Experimental aerodynamic validation of the splitter-vane TRS prototype in the LPT–OGV test rig at Chalmers University of Technology providing test data for numerical validation at GKN Aerospace Sweden.
- CFD evaluation of the splitter-vane TRS prototype and validation of the design and analysis methods by the experimental data.

2. APPROACH

The approach adopted to achieve the research objectives is explained in the following paragraphs.

At first, the aerodynamic design of a splitter-vane TRS was performed at GKN Aerospace Sweden with the help of in-house tools. The aerodynamic surfaces were then exported and handed over to Chalmers University of Technology.

At Chalmers University of Technology, the aerodynamic design was translated into mechanical design that made possible the assembly of relevant parts in the LPT-OGV rig. Once the mechanical design was defined with provisions for the planned instrumentation, the test-object was assembled in the facility and the testing of splitter-vane TRS configuration was carried out. Worth underlining that the experiments are conducted on the test-object at engine-realistic Reynolds numbers and, for the scope of this paper, only aerodynamic design point is discussed.

Finally, a numerical post-test analysis is carried out to compare the results from the experimental campaign with the industry standard numerical methods that are part of the process for design and analysis of TRS.

3. DESIGN

To date, four TRS design concepts have been tested in the LPT-OGV rig test facility at Chalmers University of Technology, and three of the configurations are shown in **Figure 1** together with schematic cross-section of the respective airfoils. These configurations were developed solely for the experimental rig and are not related to any GKN Aerospace product characteristics.

Figure 1a shows a state-of-the-art engine-realistic TRS design. The configuration is equipped with engine mounts and composed of three different vane types with radial orientation and radially varying chord (and thus varying pitch-to-chord ratio). The configuration was tested experimentally [4] and compared to numerical calculation in studies [5][6].

Figure 1b shows a design with leaned vanes, that is one of many design possibilities that can satisfy constraints from non-aerodynamic requirement. The details of experiments conducted, numerical studies and validations are found in [7][8]. The conclusion from these studies is that the aerodynamic performance in terms of total pressure loss and the functionality of de-swirling the flow could be met with lean design as well.

The third design, referred to as splitter-vane design, which is the topic of this paper, is also a lean-vane configuration but, unlike the latter that has 18 vanes, the splitter-vane design has 12 main vanes and 12 splitter vanes. The relative positioning of the splitter to the main vanes, as outcome of design experience, is shown in cross-sectional view in Figure 1c. A rigorous optimization for setting the relative position of the splitter vane was not carried out in the context of this study. The rationale behind the current splitter vane location is to minimize the rollup effect on the suction side of main vane due to pressure gradient from the pressure side of the adjacent vane.

The mid-span non-dimensional parameters for the three designs are provided in **Table 1**. It can be observed that the splitter-vane design is the most aggressive in terms of chord/pitch ratio (given for the main vanes) and max. thickness to chord ratio. As the vane designs are made more aggressive, the losses are expected to increase.

Table 1 Non-dimensional parameters of TRS Designs

	Chord / pitch	Max. thickness / chord	Number of vanes
Engine realistic	0.8	0.2	12
Lean	0.8	0.24	18
Splitter vane	1.06	0.24	12+12

As the project is focused on aerodynamic design only, it is difficult to quantify the advantages of the shorter options with respect to weight reduction. However, since the chord lengths are reduced for lean and splitter-vane TRSs, there is likely a weight advantage when manufacturing these concepts plus potential shortened engine core and nacelle, with a collateral reduced SFC of the jet-engine.

4. EXPERIMENTAL DETAILS

The experiments were carried out in the 1.5-stage LPT–OGV facility at Chalmers University of Technology, which operates at engine-representative Reynolds numbers between 100000 and 600000 based on channel height.

This facility is well suited for studies of future engine concepts such as hybrid-electric propulsion, heat recuperation, hydrogen, and effects of additive manufacturing up to TRL4, and has been developed under GKNs supervision. The test facility provides accurate and repeatable engine-representative conditions w.r.t. Reynolds numbers and flow coefficients. The presence of a rotating LPT in front of the TRS gives extra accuracy in producing wakes and flow features having, thus, the most engine-relevant conditions that a cold air test rig can provide.

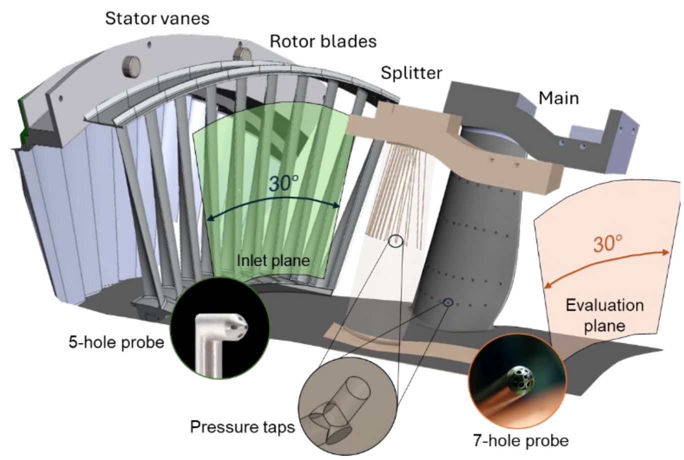

Figure 2 SCHEMATIC OF THE LPT AND TRS WITH MEASUREMENT PLANES AND INSTRUMENTATION

The rig has a shrouded LPT stage with 72 rotor blades and 60 stator vanes, designed by GKN Aerospace, providing realistic inlet boundary conditions to the downstream TRS. Further details about the facility and its design can be found in [9].

Figure 2 shows the measurement setup for the splitter-vane TRS, which includes two Outlet Guide Vane (OGV) types: main vane and splitter vane. This case is shown as an example; the same experimental procedure was used for all TRS designs considered in this study.

Total pressure and flow angle measurements were conducted using pre-calibrated five-hole probe and seven-hole probe at the inlet and evaluation planes, respectively. Both probes were automatically traversed over 30° sectors, with positioning accuracies of 0.01° circumferentially and 0.075 mm radially and axially.

For wall static pressure measurements, the main OGV was instrumented with pressure taps located at 25%, 50%, and 75% span on both the pressure and suction sides. In the splitter OGV, the reduced chord length and thickness constrained the available space for instrumentation, so pressure taps were located only at 50% span on the pressure and suction surfaces.

Pressure data were acquired with a PSI-9116 system at 500 Hz and 2.5 seconds sampling time and normalized using circumferentially averaged total ($P_{T,\mathrm{ref}}$) and static reference pressures ($P_{S,\mathrm{ref}}$) evaluated at the inlet mid-span:

$$C_{P0} = \frac{P_T - P_{T,\mathrm{ref}}}{P_{T,\mathrm{ref}} - P_{S,\mathrm{ref}}}, \quad C_P = \frac{P_S - P_{S,\mathrm{ref}}}{P_{T,\mathrm{ref}} - P_{S,\mathrm{ref}}} \quad (1)$$

The tests were performed at the on-design aerodynamic design point, typical of cruise operating condition for a narrow-body geared-turbofan engine. The average inlet swirl angle (α) was –16.9°, and the Reynolds number, based on the inlet channel height and midspan axial velocity, was 350 000.

5. NUMERICAL DETAILS

Numerical analysis of the splitter-vane design is set up similar to previously performed analyses for engine-realistic and lean-vane TRS designs [6][7][8]. A 30-degree sector with one main vane and one splitter vane is analyzed using Fluent 2023R1. The Computational Fluid Dynamics (CFD) context model with its setup is shown in **Figure 3**. The geometry was built using a commercial modelling tool and the hexahedral mesh of the model is done using ICEMCFD™. The numerical domain is extended to the Outlet plane. Surface static pressure measurements are also compared with numerical results.

Steady-state Reynolds-averaged Navier–Stokes (RANS) simulations are performed, and a correlation-based transition-SST turbulence model is used. The model is based on two transport equations (γ–θ model), one for the intermittency and one for the transition onset criteria in terms of momentum thickness Reynolds number. The detailed model definition can be found in the publication by Menter et al. [10].

The numerical analysis uses the experimental data from the 5-hole probe at the Inlet plane (**Figure 2**) as inlet boundary condition.

A full-wheel contour is derived from the measurements of a 30-degree sector and imposed at the inlet of the CFD domain. The total pressure contour is shown in **Figure 4**. The total pressure distribution is tip strong with traces of wakes from upstream Nozzle Guide Vanes (NGVs). Since the wakes from upstream NGVs are seen in the contour, the clocking position of splitter-vane geometry with respect to these stator wakes becomes important. Accordingly, the clocking position of the numerical domain is matched to the clocking position of the test rig. Total pressure values at end-walls are assumed to be the same as the measured static pressure values closest to end-walls (≈15% span from hub and ≈5% span from shroud). This approach was studied by Nylander et al. [6] and the same method is used in the present analyses for extrapolating the missing data from the experimental measurements due to the interference of the instruments with the end walls.

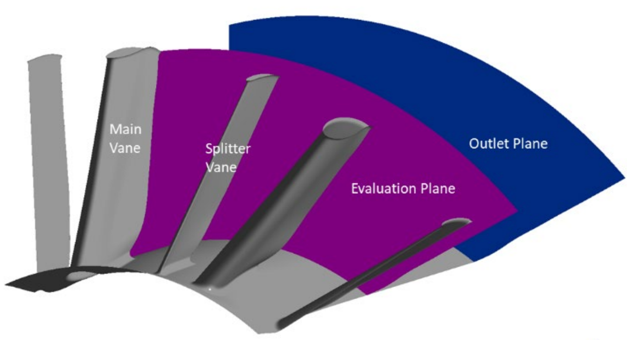

Figure 3 NUMERICAL SETUP (TWO SECTORS OF THE FULL-WHEEL CFD DOMAIN)

The flow angle variation that was measured at the inlet of the TRS is used for numerical simulations as boundary condition is also shown in **Figure 4**. The inlet swirl angle varies spanwise from –40° at the hub to around 0° (axial flow) at the shroud. A TRS is expected to de-swirl this inlet flow and maximize the axial momentum. De-swirling is also necessary to minimize mixing losses when the core-flow mixes with bypass flow.

The turbulence intensity at the inlet is specified as 5% while the turbulent length scale is set to 0.0012 m [11]. This turbulent length scale is based on internal validation effort that provides acceptable comparison with test data. The intermittency parameter is retained as the default value and is equal to 1.

5.1 Mesh sensitivity study

A mesh sensitivity study has been performed to find a satisfactory number of nodes for numerical prediction for single sector configuration. Three meshes, called M1, M2 and M3, corresponding to 2.4 million, 4.8 million and 7 million nodes respectively, were created and analyzed. The variation of mass flow averaged C_{p0} numbers at evaluation plane, shown in **Figure 5**, is considered as criteria for selecting the appropriate number of nodes.

It can be observed that there is no considerable difference in C_{p0} between the three meshes. From these simulations, M2 was chosen to provide good balance in computing accuracy and speed, and hence, results from M2 are reported in the present work.

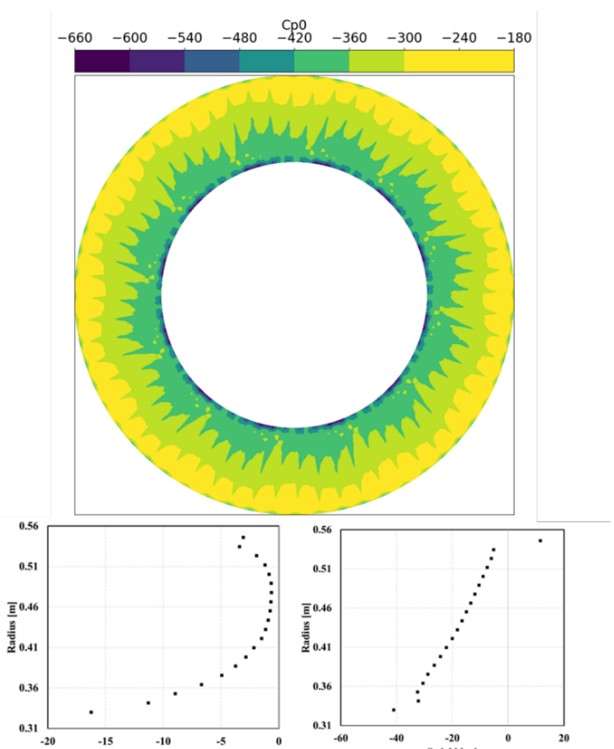

Figure 4 INLET BOUNDARY CONDITIONS FOR SPLITTER-VANE TRS

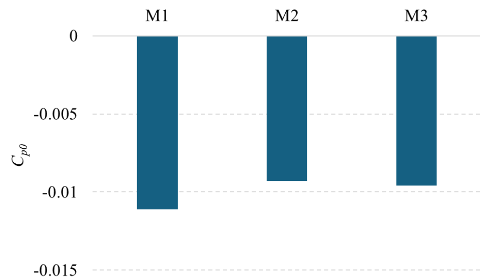

Figure 5 IMPACT OF NUMBER OF NODES ON NUMERICAL PREDICTION

With the background information provided herein, the results of the study will be discussed in following sections. Results will be discussed first by comparing only experimental data for three TRS design configurations. After experimental comparison, numerical results will be compared to experimental results for splitter-vane design only. Numerical comparison with engine-realistic and lean-vane designs are presented in previous publications [6][8].

6 RESULTS AND DISCUSSION

6.1 Blade-loading comparison

Normalized static pressure (C_p) distribution along the chord of OGVs at three spanwise locations are compared in **Figure 6**. The first row of plots shows experimental blade-loading comparisons for the three different TRS designs. In the second row, blade-loadings are compared between experiments and CFD for the splitter-vane design only. The leading edges of vanes in **Figure 6** are not matched. Instead, the explicit axial coordinates are shown in the plots to highlight the differences of their respective positions in the three different TRS designs (i.e. engine realistic, lean vane, splitter vane). To begin with, few observations from experiments are presented.

When examining **Figure 6** from left to right (25% span to 75 % span), it is possible to notice a decrease in the loading at each span. This happens because the inlet flow imposed on the TRS presents a high swirl angle near the hub while gradually, and almost linearly, reaches an axial flow near the shroud. Hence, the vane has to perform more flow de-swirling at lower span (higher loading), than in the upper span (lower loading).

Together with the inlet swirl angle, the maximum thickness of the vane plays a crucial role in the distribution of the static pressure on the vane. The engine-realistic configuration, with the lowest maximum-thickness to chord ratio (**Table 1**), has a lower gradient of acceleration and diffusion at suction side. On the other hand, both lean-vane and splitter-vane designs, due to their larger maximum-thickness to chord ratios, have a high gradient of acceleration and diffusion, and the effect is consistent for all the plotted spans.

The airfoil geometry for the vane in the lean-vane design is identical to the main vane in the splitter-vane design. However, while the lean-vane TRS has 18 vanes, the splitter-vane TRS has 12 pairs of main and splitter vanes. Considering the difference in blade count, it can be expected to see higher aerodynamic loading in the main vane of the splitter-vane TRS than in the lean-vane one. Contrary to expectations, the main vane in the splitter-vane TRS experiences lower loading. This happens because both the main and the splitter vanes have a de-swirling function, thus the load is shared between the two. Consequently, the combined blade-loading in the main and splitter vanes cover a larger area compared to blade-loading in the lean-vane design.

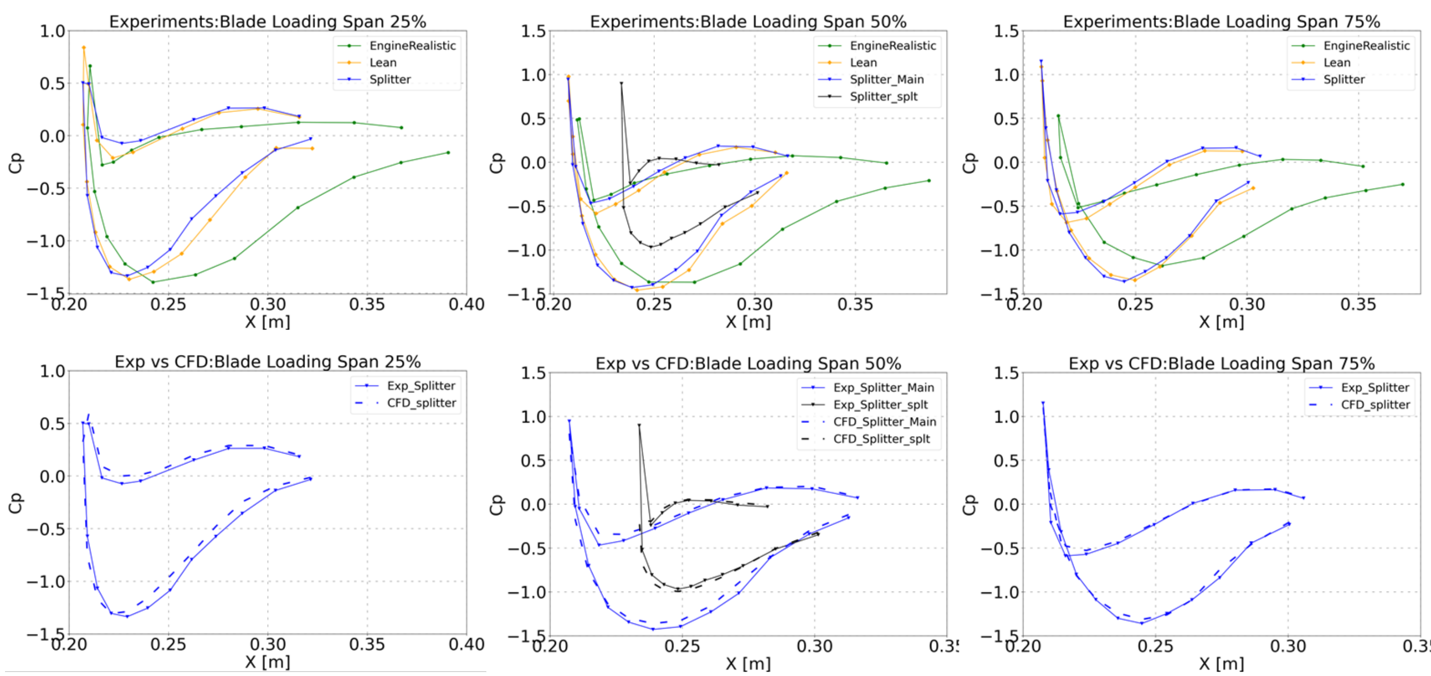

Figure 6 BLADE-LOADING PLOTS

This effect becomes visually evident at 50% span, where static pressure measurements on the splitter vane are also plotted alongside other TRS designs. The overall blade-loading in the splitter-vane design is the composition of the blue (main-vane in splitter-vane design) and black curves (splitter vane in splitter-vane design). It should be noted that blade-loading measurements for the splitter vane are available only at 50 % span.

Focusing on the comparison between experimental measurements and CFD results for the splitter-vane design(bottom row of **Figure 6**), the numerical static pressure values are extracted at same point locations as in the experiments. To evaluate the accuracy of CFD in replicating the experimental data, three key aspects are considered: acceleration and diffusion on the vane suction side, and incidence. It can be observed that CFD, with the current setup, captures all three aspects with satisfactory accuracy.

As a closing remark on blade-loading plots, the chord length reduction in the lean and splitter-vane designs is approximately 0.08 m. This reduction enabled the development of separation-free designs that are able to de-swirl the inlet flow effectively, highlighting the potential of such designs. However, because of the higher diffusion observed in lean and splitter-vane TRSs, additional losses are introduced within the flow passage, which become evident at the evaluation plane for all three configurations. Next, a discussion on total pressure losses distributions at the evaluation plane is presented.

6.2 Normalized Total Pressure at Evaluation Plane

The normalized total pressure (C_{p0}) distribution at the evaluation plane (**Figure 3**) for the three designs is presented in **Figure 7**. The first row shows contours obtained from experimental measurements, while the second row displays contours from numerical analyses. For the engine-realistic design, the CFD contours are taken from the work done by Nylander et al. [6], and for the lean-vane design, from Deshpande et al. [8]. CFD simulations for the splitter-vane design are performed as part of the present study.

The engine-realistic and splitter-vane designs have periodicity of 30°, while the lean-vane design has periodicity of 20°. However, measurements were conducted over a 30° sector for all TRS configurations; therefore, all contours presented in **Figure 7** correspond to 30° sectors. The evaluation planes are located at identical axial locations downstream of the vane trailing edge for all TRS designs. In terms of wake distribution, the engine-realistic case has 12 wakes, the lean-vane design 18 wakes, and splitter-vane design 24 wakes comprising of 12 main-vane wakes and 12 splitter-vane wakes.

Distinct wakes from TRS vanes are clearly visible, along with smaller wavelength total pressure peaks. These peaks originate from the upstream NGVs, whose wakes propagate through the rotor and TRS vanes, becoming clearly visible at the evaluation plane. Additionally, regions of lower C_{p0} values and loss inducing secondary flows are more pronounced at lower spans, primarily due to higher blade-loading and increased need for flow turning in these regions.

The formation of passage vortices at lower spans of a TRS vane is explained by Deshpande et al. [8]. Passage vortices are seen in all three configurations, with their radial migration governed by local pressure gradients in both tangential and radial directions. Among the designs, radial migration is least in the engine-realistic design, while the lean and splitter-vane designs exhibit passage vortices at relatively higher radii. In the splitter-vane design, additional passage vortices are generated by the splitter vanes, resulting in a total of 24 vortices: 12 from the main-vanes and 12 from the splitter-vanes.

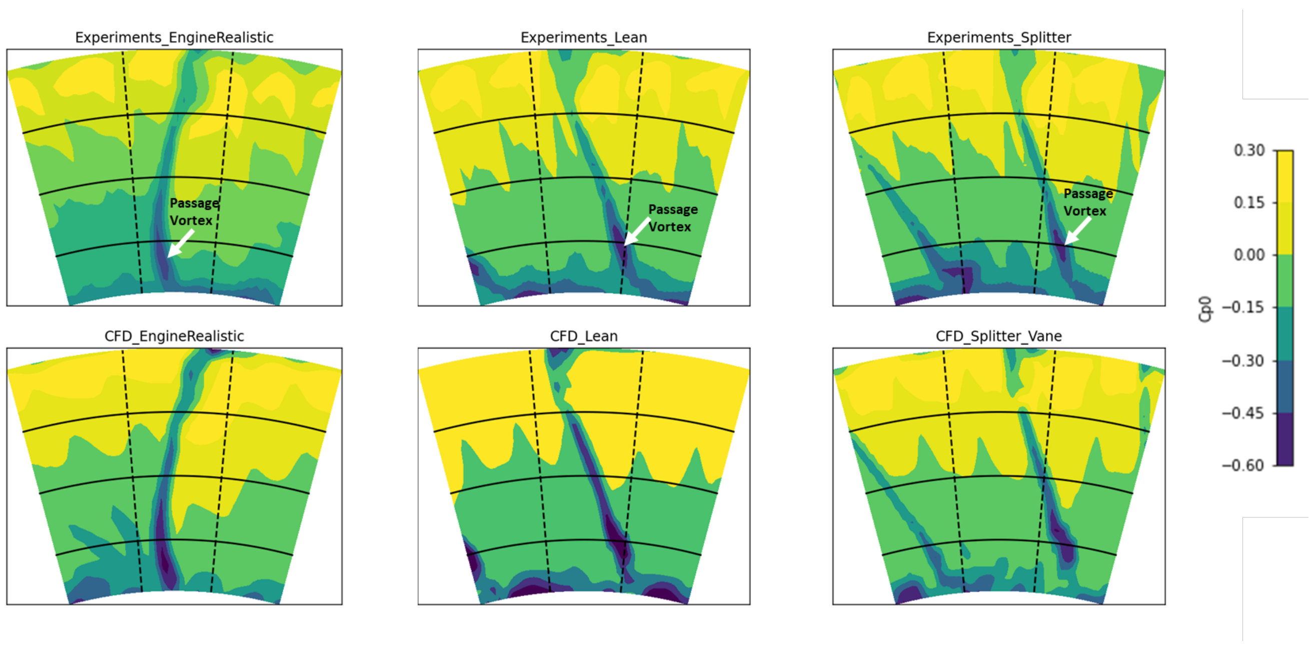

Figure 7 COMPARISON OF C_{P0} CONTOURS AT EVALUATION PLANE

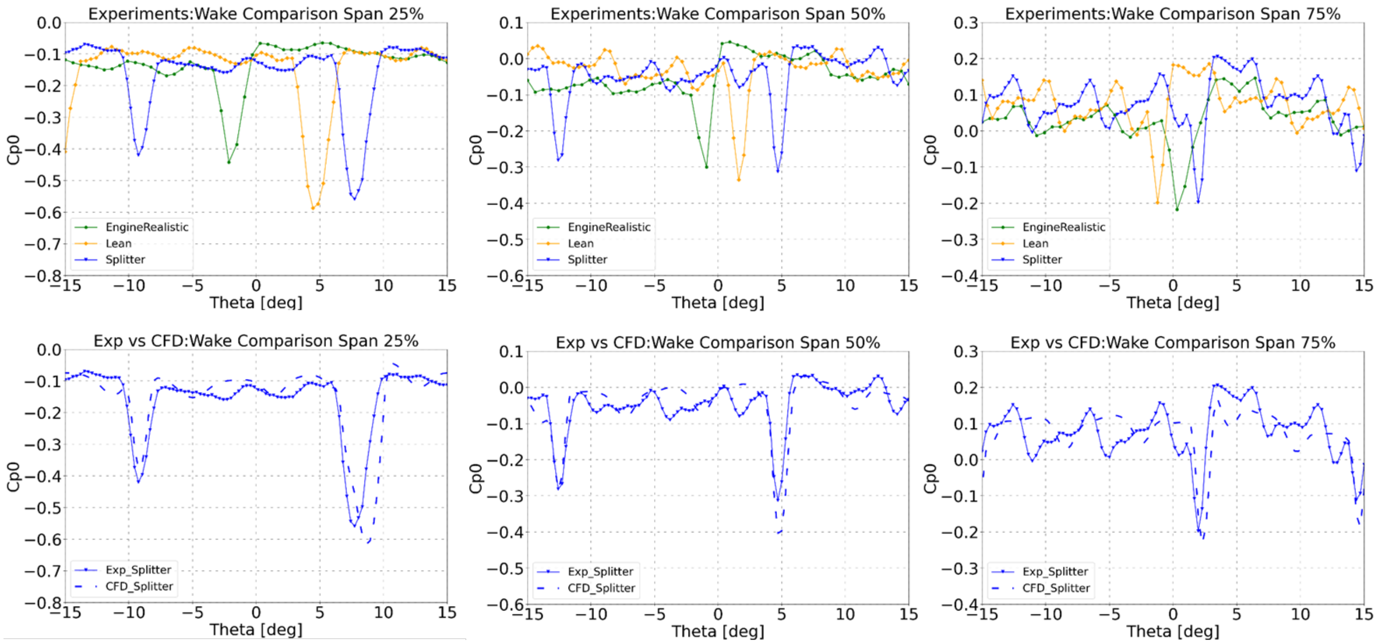

Figure 8 WAKE PLOTS AT THREE SPANS

For comparison, the engine-realistic configuration has 12 vortices, and the lean-vane configuration has 18, as expected by the different vane count of each design. The passage vortex formed by the splitter-vane is comparable in size to those from the main vane. Since the passage vortices are considered loss inducing sources and also considering the number of such features for each design, the splitter-vane TRS is expected to produce higher losses than the engine-realistic TRS, with the lean-vane TRS falling in between.

Comparison of experimental contours with CFD results reveal that the latter accurately captures the flow structures observed in the experiments and the loss regions in CFD align well with the measurements, confirming the suitability of this simulation approach for use during design phases and pretest analyses. The close agreement in vortex positioning between CFD and experiments also validates the correct clocking of the OGV vanes applied in the numerical analyses. Furthermore, the influence of NGV wakes is evident in the CFD contours, as the contour of inlet boundary condition incorporates NGV-induced effects.

Tangential and radial reference lines are marked on the contours to facilitate comparison of flow structure locations between experiments and CFD. The tangential lines correspond to 25%, 50% and 75% span positions. In the next section, two-dimensional plots of C_{p0} along these tangential lines, commonly referred to as wake plots, will be discussed to further estimate total pressure losses.

6.3 Wake plots at three spans

Figure 8 illustrates C_{p0}-distributions along tangential lines (as defined in **Figure 7**) at three spanwise locations, 25%, 50%, and 75%, on the evaluation plane. Consistent with the previous sections, the first row of **Figure 8** presents experimental data, while the second row compares experimental and numerical data of the splitter-vane design only. Wake locations exhibit tangential variation across different TRS designs, with the engine-realistic configuration displaying the smallest wake depths. Both wake depth and wake width are critical contributors to losses for a given design configuration.

More in detail, at respectively 25% and 50% span, the engine-realistic TRS shows a narrower wake width compared to the other two designs. At 75% span, however, the wake of engine-realistic design overlaps with NGV-originated wakes, thus making a direct comparison of wake widths of the other two designs impractical at this location. The larger wake width observed in the lean and splitter-vane configurations can be directly attributed to their higher maximum thickness-over-chord ratios, as reported in **Table 1**.

From the wake plots in **Figure 8**, one can clearly identify azimuthal locations affected by wake flow, while the remaining regions can be considered nearly loss-free. These angular extents of wakes are multiplied by the number of vanes to compute the total wake width over 360°, as presented in **Figure 9**. In line with expectations, the engine-realistic design has the least total wake width. The lean-vane design shows a relatively larger wake width, while the splitter-vane design, by virtue of its thick, short vanes and additional splitter vanes, results in the highest wake width.

Given that the splitter-vane design exhibits the largest wake width, and therefore the smallest of clean flow at the evaluation plane, the total pressure loss for this configuration is expected to be the highest among the three design options.

When assessing the capability of numerical methods to capture wakes, three aspects become crucial: wake width, wake depth, and wake location [8]. For the splitter-vane design, the

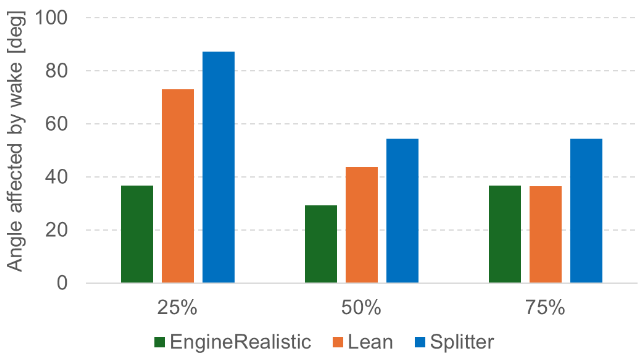

Figure 9 FLOW AFFECTED BY WAKE

comparison between experimental and CFD wake features indicate that the numerical predictions are acceptable. Wake depths are slightly overpredicted in CFD, and wake locations show a minor offset of approximately 1.5°. Given the experimental uncertainty of 0.01 counts in *Cp0*, the agreement between CFD and experimental measurements is deemed satisfactory. Therefore, the numerical method employed is considered reliable for predicting flow in splitter-vane TRS configurations.

Building on the observations in this section regarding total pressure losses associated with secondary flow and wake-induced effects, the next session will examine the overall losses.

6.4 TRS Total pressure loss

Total pressure values are averaged at both inlet and the evaluation plane of the TRS. The difference in total pressure between these two planes is normalized by inlet dynamic head and reported as loss coefficients. These loss values are presented as delta losses relative to engine-realistic TRS configuration, as shown **Figure 10**.

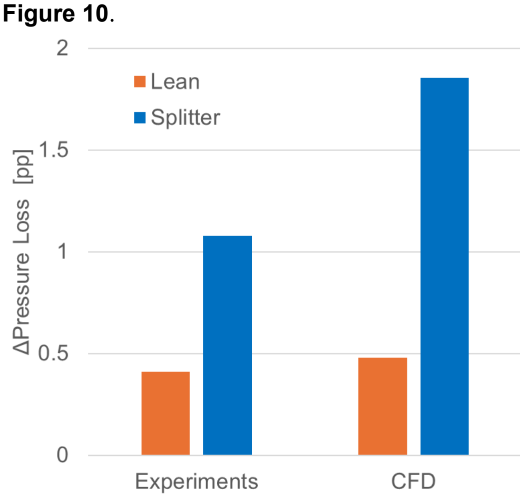

Figure 10 TOTAL PRESSURE LOSS

The lean-vane TRS design shows higher losses when compared to engine-realistic design, while the splitter-vane configuration exhibits the highest losses. This trend in total pressure loss, noticed in both experiments and CFD, can be related to non-dimensional design parameters listed in **Table 1**. The engine-realistic configuration, as the name suggests, was intended to replicate a legacy TRS geometry in an engine. In contrast, the lean-vane design was made more aggressive by reducing the vane axial length while maintaining the chord-to-pitch ratio of the engine-realistic design through an increased number of vanes. Additionally, the lean-vane design features a higher thickness-to-chord ratio (0.24 versus 0.20). The combination of reduced chord and increased thickness-to-chord ratio contributed to the increased losses observed for the lean-vane design.

In the splitter-vane design, the chord-to-pitch ratio was reduced and the thickness-to-chord ratio increased compared to the engine-realistic configuration. It is important to note that only the main vanes in the splitter-vane design were considered for calculating the non-dimensional parameters. This design was made more aggressive in two steps: by increasing the chord-to-pitch (lighter TRS) and by increasing the maximum thickness (shorter TRS). These changes result in additional losses when compared to both engine-realistic and lean-vane designs.

The high losses observed in the splitter-vane configuration were anticipated based on the C_{p0} contours in **Figure 7** and the wake plots in **Figure 8**. The presence of multiple passage vortices contributed to secondary losses, while the large wake width significantly increased primary losses in this design. These higher wake widths are a direct outcome of the higher diffusion factors evident in the blade-loading plots shown in **Figure 6**.

The purpose of introducing a splitter vane was to improve flow guidance and assist in turning the flow with a reduced vane count. The reduced vane count and shorter vanes of the splitter-vane TRS permits manufacturing both lighter and shorter TRS. The pay-off for the shorter and lighter TRS is marginally increased losses, both in terms of secondary and primary losses.

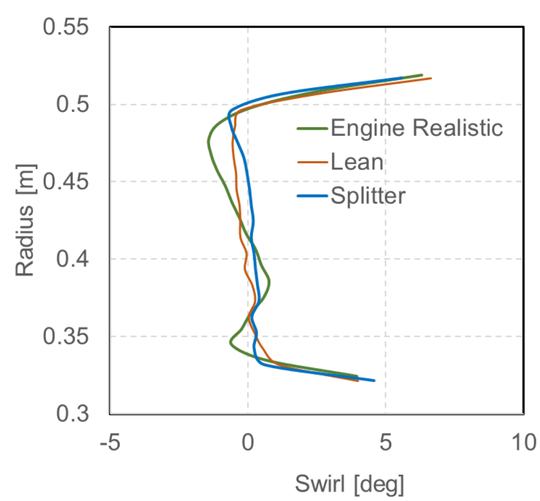

Figure 11 RADIAL PROFILES OF SWIRL AT TRS EXIT

6.5 Aerodynamic Functionality of TRS

The primary aerodynamic function of a TRS is to de-swirl the LPT outlet flow and align it axially. The swirl present at the TRS inlet is shown in **Figure 4**, while the swirl values of flow exiting the TRS are shown in **Figure 11**.

All three TRS designs successfully de-swirl the flow to nearly 0°, fulfilling the intended aerodynamic function. Anyhow, the lean and splitter-vane configurations achieve this close to zero bulk outlet flow angles at the cost of higher total pressure losses. Furthermore, the lean-vane and splitter-vane designs can result in a lighter and shorter TRS, thus potentially resulting in a lighter jet-engine with a shortened core and nacelle, thus lower SFC.

7 CONCLUSIONS

The study paves the way for a next-generation, ultra-short engine architecture by delivering a novel splitter-vane based TRS design with short length and possibly reduced weight. Among the turbofan engine components, the TRS and its interface with the LPT have been identified as one of the areas for aerodynamically aggressive design. A shortened TRS offers multiple advantages: improved fuel efficiency due to a more compact engine core and nacelle, reduced engine weight, enhanced rotor dynamics from a shorter shaft, and improved airframe integration. In addition, the splitter-vane concept enables design flexibility for future hybrid-electric engines, where the TRS must allow routing of electrical cables.

Achieving such aggressive designs requires validated aerodynamic performance data for achieving the needed prediction accuracy of design tools used at GKN Aerospace. Aggressive configurations operate closer to flow-separation limits, which requires CFD methods to be validated. The validation effort helps improve predictability and reliability of CFD methods.

In this work, the radical splitter-vane TRS concept has been designed at GKN Aerospace, and manufactured, assembled, and tested at TRL 4 in the world-unique Chalmers LPT–OGV test rig. The study explores design spaces never studied before and delivers the first experimental validation database for novel aerodynamically aggressive TRS configurations incorporating splitter vanes. It also provides the validation of numerical tools for this configuration, thereby reducing future design risks.

The splitter-vane TRS is compared directly against two engine-realistic state-of-the-art GKN designs: one with radial vanes and one with leaned vanes. All three configurations were developed at GKN and tested at the Chalmers LPT–OGV facility. Both experimental and CFD results show that the splitter-vane TRS achieves the required flow-straightening performance, producing marginally increased losses. The additional losses originate from a combination of higher diffusion (confirmed by blade-loading analysis), wider wakes, and a larger number of passage vortices. These findings highlight opportunities for further optimization of vane placement and geometry, particularly when combined with additive manufacturing methods. Additive manufacturing methods remove many of the constraints present in this study and offer a significant potential for optimization in terms of splitter vane location and shape.

Despite the increased total pressure losses in the current splitter-vane design, its reduced chord length offers potential engine weight reduction advantages. While the 18 struts lean-vane design also reduces the chord, it incorporates 18 vanes, whereas the splitter-vane with 12 main vanes and 12 splitter vanes configuration could result in lower overall weight, providing the greatest potential benefit in terms of improved SFC. However, since the present study focuses exclusively on aerodynamic performance, such weight-related advantages cannot yet be fully claimed.

From an aerodynamic standpoint, all three TRS configurations demonstrate the ability to de-swirl the LPT exit flow to near-zero angles with acceptable losses. The industry-standard CFD methodology successfully used here accurately predicts key features such as blade-loading, wake development, and secondary flow structures.

ACKNOWLEDGEMENTS

The project is supported by Clean Aviation Joint Undertaking and its members. Additional funding is provided by GKN Aerospace Sweden AB and Vinnova/NFFP. The authors acknowledge the Chalmers Laboratory of Fluids and Thermal Sciences for hosting the facility and providing measurement equipment.

CLEAN AVIATION

Co-funded by the European Union

Disclaimer: Funded by the European Union. Views and opinions expressed are however those of the authors' only and do not necessarily reflect those of the European Union or the Clean Aviation Joint Undertaking. Neither the European Union nor the granting authority can be held responsible for them.

REFERENCES

[1] Youngren, H.H. "Analysis and design of transonic cascades with splitter vanes". *M.S. thesis. Massachusetts Institute of Technology*, 1991.

[2] Clark, C.J., Pullan, G., Curtis, E., and Goenaga, F. "Secondary flow control in low aspect ratio vanes using splitters." ASME. *J. Turbomeca*. 2017; 139(9): 091003. https://doi.org/10.1115/1.4036190

[3] Yasa, T., Lavagnoli, S. and Paniagua, G. "Impact of a multi-splitter vane configuration on the losses in a 1.5 turbine stage." *Proceedings of the Institution of Mechanical Engineers, Part A: Journal of Power and Energy*. 2011; 225(7): 964-974.https://doi.org/10.1177/0957650911409843

[4] Vikhorev, V. and Chernoray, V. "Experimental flow analysis in a modern turbine rear structure with 3D polygonal shroud under realistic flow conditions." *Proc. of 14th European Turbomachinery Conference on Turbomachinery Fluid Dynamics and Thermodynamics*, *ETC 2021*.

[5] Vikhorev, V., Nylander, P., Chernoray, V., Larsson J., and Thulin, O. "Experimental and numerical flow analysis of an engine-realistic state-of-the-art turbine rear structure."

ASME. *J. Eng. Gas Turbines Power*. 2022; 144(7): 071009. https://doi.org/10.1115/1.4054075
[6] Nylander, P., Deshpande, S., and Larsson, J. “Influence from nozzle guide vane wakes and inlet end-wall boundary layers on turbine rear structure aerodynamics.” *Proc. of the ASME Turbo Expo 2022,* Vol. 10C. V10CT32A018, https://doi.org/10.1115/GT2022-81677
[7] Vikhorev, V., Chernoray, V., Abdel-Mallak, Z., and Larsson, J., “The influence of the vane lean on the flow in a turbine rear structure”. *Proc. of Congress of the International Council of the Aeronautical Sciences* (ICAS), 2022.
[8] Deshpande, S., Ricchi, M., Larsson, J., Vikhorev, V., and Chernoray, V. “Impact of lean on aerodynamic performance of a turbine rear structure.” *Proc. of the ASME Turbo Expo 2024*, Vol. 12C, V12CT33A005. https://doi.org/10.1115/GT2024-122626
[9] Rojo, B., “Aerothermal experimental investigation of LPT-OGVs”, *PhD Thesis, Chalmers University of Technology*, Gothenburg, Sweden, 2017.
[10] Menter, F.R., Langtry, R.B., Likki, S., Suzen, Y., Huang, P., and Völker, S. “A correlation-based transition model using local variables—part I: model formulation.” ASME *J. Turbomach.* (2004): 413-422. https://doi.org/10.1115/1.2184352
[11] Jonsson, I., Chernoray, V., and Rojo, B. “Surface roughness impact on secondary flow and losses in a turbine exhaust casing.” Proc. of the ASME Turbo Expo 2018, Vol. 2B, V02BT41A009. https://doi.org/10.1115/GT2018-75541 .

